Eur. Phys. J. B **35**, 317–323 (2003)
DOI: 10.1140/epjb/e2003-00283-3

THE EUROPEAN PHYSICAL JOURNAL B

A magnetic study of the one dimensional Sr_3NiIrO_6 compound

D. Flahaut[1], S. Hébert[1], A. Maignan[1,a], V. Hardy[1], C. Martin[1], M. Hervieu[1], M. Costes[2], B. Raquet[2], and J.M. Broto[2]

[1] Laboratoire CRISMAT, UMR CNRS ISMRA 6508, 6 boulevard du Maréchal Juin 14050 Caen Cedex, France
[2] Laboratoire National des Champs Magnétiques Pulsés, LNCMP, avenue de Rangueil, 31432 Toulouse, France

Received 28 April 2003 / Received in final form 21 July 2003
Published online 15 October 2003 –

Abstract. The magnetic properties of a polycrystalline Sr_3NiIrO_6 sample have been investigated by means of susceptibility and magnetization measurements. On the one hand, it is found that this compound, made of magnetic chains on a triangular lattice, behaves very similarly to Ca_3CoRhO_6 and Ca_3CoIrO_6. In particular, at low temperature ($T < T_2$ (= 21 K)), a frozen state, characterized by a very slow spin dynamic, is evidenced. On the other hand, for $T_2 < T < T_1$ (=70 K), this phase exhibits magnetization values, smaller than the expected ones, with a 1/3 plateau reminiscent of the ferrimagnetic state of Ising spins on a triangular lattice. Nonetheless, the absence of saturation in 35 T and the low magnetization values are consistent with an antiferromagnetic intrachain coupling between Ir^{4+} ($S = 1/2$) and Ni^{2+} ($S = 1$). Sr_3NiIrO_6 can be viewed as made of antiferromagnetically coupled ferrimagnetic chains on a triangular lattice. On the basis of these results, a magnetic (H, T) phase diagram is proposed.

PACS. 75.30.Cr Saturation moments and magnetic susceptibilities – 75.10.Pq Spin chain models – 75.30.Gw Magnetic anisotropy

The one-dimensional $Ca_3Co_2O_6$ compound is an illustrative model [1,2] of the numerous fascinating magnetic properties exhibited by the transitions-metal oxides. This phase belongs to a wide family of compounds [3] crystallizing in the K_4CdCl_6 structure with chains built of alternative trigonal prisms and octahedra sharing a triangular face. In $Ca_3Co_2O_6$, the Ca cations ensures the cohesion between chains, and in the latter, the trivalent cobalt adopt two different spin states, high-spin (H.S.) and low-spin (L.S.) in the trigonal prisms and octahedra, respectively [2,4]. With this $S = 2/S = 0$ spin-state ordering, a ferromagnetic intrachain coupling with colinear magnetic moments along the chain is found whereas the interchain coupling is antiferromagnetic [4]. Perpendicularly to the chains, the cobalt cations form a buckled triangular lattice, and thus the projection of the ferromagnetic moments of each chain on this plane can be compared to an Ising triangular lattice [5]. More recently, it has been shown that the partially disordered antiferromagnetic (PDA) state, theoretically predicted by Mekata *et al.* [6], was realized in the isostructural Ca_3CoRhO_6 compound [7]. The theoretical model was initially proposed to explain the magnetic properties of hexagonal $CsCoCl_3$ and $CsCoBr_3$ quasi-one-dimensional $S = 1/2$ Ising like antiferromagnets characterized by a triangular array of magnetic chains with both intra-and interchain antiferromagnetic coupling. Upon cooling, in between T_1 and T_2, the PDA state is realized, 2/3 of the magnetic chains order antiferromagnetically whereas the 1/3 remaining one looses its magnetic coherence along the chain.

In the Ca_3CoRhO_6 compound, the H.S. Co^{2+} (or Co^{3+}) and L.S. Rh^{4+} (or Rh^{3+}) cations are located in the trigonal prism and octahedra, respectively [7,8]. As this compound is cooled down between $T_1 = 90$ K and $T_2 = 32$ K, the PDA state is also realized [7]. But it should be emphasized that in contrast to the intrachain antiferromagnetic coupling of $CsCoCl_3$, the intrachain coupling is ferromagnetic in Ca_3CoRhO_6. Among the $A_3BB'O_6$–type compounds, three of them, Ca_3CoRhO_6 [8], Ca_3CoIrO_6 [9] and Sr_3NiIrO_6 [10] have been reported to exhibit the same kind of magnetic behavior from dc magnetization measurements. They exhibit two characteristic temperatures, T_1 and T_2, with a decrease of the magnetic susceptibility below T_2 leading to a magnetic susceptibility such as $\chi\ (T \to 0) \sim 0$ in zero-field-cooling mode. It should be pointed out that a T_2 temperature is also observed for $Ca_3Co_2O_6$ but with no such $\chi\ (T \to 0) \sim 0$ feature [1–4]. If one considers the chemical formulas of these 1D compounds, it is remarkable that for A = Sr, B = Ni^{2+} and B' = Ir^{4+} this kind of magnetic behavior is also observed although the spacing between nearest chains is increased as one goes from Ca^{2+} to Sr^{2+} and furthermore that Ni^{2+} is not isoelectronic to Co^{2+}. In the present paper, we report on a magnetic study of Sr_3NiIrO_6 by means of

[a] e-mail: antoine.maignan@ismra.fr

ac-susceptibility and magnetization measurements. By comparing these data to those obtained for Ca_3CoRhO_6, it is found that a frozen state is observed below $T_2 = 21$ K in Sr_3NiIrO_6 which mimics the frozen PDA state reported for Ca_3CoRhO_6 [7,8]. A remarkably slow spin dynamic is evidenced by the relaxation study of the dc magnetization, just below T_2, which fitting is consistent with a model used for conventional spin glasses [11]. In contrast to Ca_3CoRhO_6, Ca_3CoIrO_6 and $Ca_3Co_2O_6$, in between T_1 (= 70 K) and T_2 (= 21 K), the magnetization does not saturate even in 35 T which strongly supports an intrachain antiferromagnetic coupling between Ni^{2+} and Ir^{4+}. A magnetic phase (*H, T*) diagram is proposed for Sr_3NiIrO_6.

Experimental

Polycrystalline samples were prepared *via* solid state reactions. The compound, starting from stoichiometric mixtures of $SrCO_3$, NiO and IrO_2, was calcinated in air at 800 °C, 900 °C and 1000 °C for 24 h. Then the product was pressed in the form of bars under 1 ton/cm^2 and heated at 1150 °C for two weeks with intermediate grindings. It was finally cooled down to room temperature (RT) at a speed of 100°Ch^{-1}. Powder of the reacted bars was characterized at RT by using a Philips X-ray diffractometer using CuKα (from 10 to 100° in 2θ with steps of 0.02). Lattice parameters were obtained from the Rietveld analysis of the X-ray data [12]. Sample for electron microscopy study was prepared by smoothly crushing the crystallites in alcohol. The small flakes were deposited on a holey carbon film, supported by a copper grid. Electron diffraction (ED) and energy dispersive spectroscopy (EDS) characterizations were carried out at room temperature with a JEOL 200CX electron microscope equipped with KEVEX analyser. The reconstruction of the reciprocal space was carried out by tilting around crystallographic axes.

Magnetization measurements were performed with magnetometers working with maximum magnetic fields of either 5 T or 9 T. After each magnetic field setting, a pause of 30 s. was made prior to the measurement. A 40 T pulsed magnetic field using the facilities of the Laboratoire National des Champs Magnétiques Pulsés of Toulouse has also been used to measure the magnetization. For the latter technique, the typical duration of a magnetic sweep from 0 to 40 T is of sec. Alternative current (ac) susceptibility (χ) as a function of temperature was collected with a Quantum Design susceptometer by using an ac magnetic field 3 Oe with frequencies between 1 Hz and 1 kHz and without applying a dc magnetic field.

Results

Structural features

The investigation of about fifty crystallites showed a slight deviation of the actual cationic composition of the sample with regard to the nominal one. The Sr/(Ni+Ir) ratio is highly constant (= 3/2) and the average cation content is $Sr_3Ni_{1.1\pm0.04}Ir_{0.9\pm0.04}$. The ED study leads to cell parameters of $a \sim 9.6$ Å and $c \sim 11$ Å and symmetry consistent with the space group R $\bar{3}$ c. The spots are sharp, confirming the good crystallinity of the sample.

Structure refinements of Sr_3NiIrO_6 from X-ray diffraction data were thus performed in the space group R $\bar{3}$ c (N° 167). The refined cell parameters, $a = 9.6066(1)$ Å and $c = 11.1748(2)$ Å, are in agreement with those previously reported [10]. Note that oxygen stoichiometry has not been checked. The structure consists of one-dimensional chains of alternating face-sharing IrO_6 octahedra and NiO_6 trigonal prisms. The chains are separated by the strontium cations.

Physical properties

Paramagnetic state: nature of the intrachain magnetic coupling

As one considers the properties of Sr_3NiIrO_6, a first question arises about the electronic configurations of the BB' cations involved in this $A_3BB'O_6$ phase. From the temperature dependence of the inverse magnetic susceptibility (Fig. 1), an effective number of Bohr magnetons (μ_{eff}) can be extracted from the Curie constant C, by fitting the $\chi(T)$ curve with a Curie-Weiss law of the type $\chi = \frac{C}{T-\theta_p}$. The obtained experimental value, μ_{eff} =3.4μ_B is close to the calculated value $\mu_{calc.} = 3.32\mu_B$/f.u. obtained for a combination of high spin Ni^{2+} ($S = 1$) and low-spin Ir^{4+} ($S = 1/2$). Note that a mixture of trivalent species, Ni^{3+} ($S = 1/2$) and Ir^{3+} ($S = 0$) leads to a much smaller value. At that point, it is important to mention that in the absence of high oxygen pressures, the most stable oxidation is divalent for Ni whereas the tetravalent oxidation state is the most stable for iridium (Ir (III) is only stabilized in Sr_3TaIrO_6 and Sr_3NbIrO_6 [13]). Furthermore, in an oxygen lattice, due to the large increase of the 10 Dq value, as one goes from 3*d* to 5*d* cations, the most stable spin state for Ir^{4+} at low temperature is low-spin. The chain can thus be described as alternating $S = 1$ and $S = 1/2$ magnetic moments. This situation differs from the proposed $S = 2$ and $S = 0$ alternated moments in the chain for $Ca_3Co_2O_6$ and from the $S = 3/2$ and $S = 1/2$ spin-states for H.S. $Co^{2+}$and L.S. Ir^{4+} (or Rh^{4+}) in the case of Ca_3CoIrO_6 and Ca_3CoRhO_6.

From the χ^{-1}(T) curve of Figure 1, it turns out that the θ_p value of Sr_3NiIrO_6, $\theta_p \sim -61$ K, is negative in contrast to the positive values reported for $Ca_3Co_2O_6$ ($\theta_p = 80$ K, [2]), Ca_3CoRhO_6 ($\theta_p = 150$ K, [8]) and Ca_3CoIrO_6 ($\theta_p = 160$ K [9], see also the curve in Fig. 1). This indicates that antiferromagnetic fluctuations at high temperature dominate in the case of Sr_3NiIrO_6. This difference becomes clearer as one looks at the deviation from the $\chi^{-1}(T)$ linearity, upwards for the $Ca_3BB'O_6$ (B = B' = Co; B = Co and B' = Ir or Rh) with large and positive θ_p values but downwards for Sr_3NiIrO_6 together

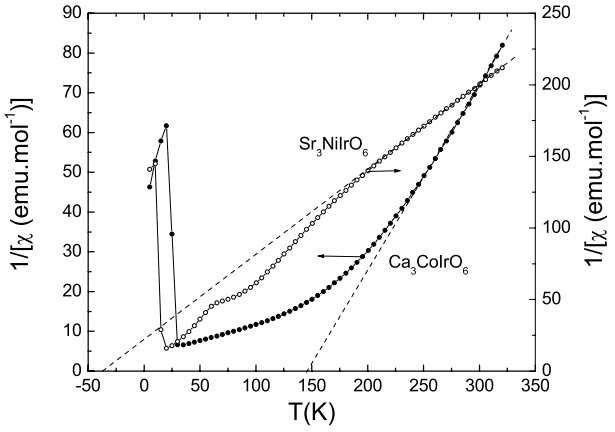

Fig. 1. T dependence of the inverse magnetic susceptibility [$\mu_0 H = 0.3$ T] for Sr_3NiIrO_6. The $\chi^{-1}(T)$ curve of Ca_3CoIrO_6 is also shown for comparison.

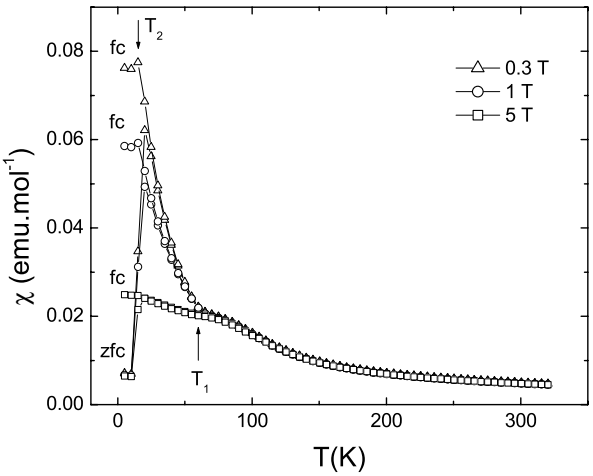

Fig. 2. T dependence of the magnetic susceptibility χ. The data are deduced from M data collected upon warming in zero-field-cooling (zfc) and field-cooling modes (fc). The magnetic field values are indicated on the graph. The characteristic temperature T_1 and T_2 are shown by arrows

with a negative θ_p. From this observation, it turns out that the intrachain coupling is negative leading to a net ferrimagnetic magnetization along the chains with alternating antiferromagnetic $S = 1$ and $S = 1/2$ magnetic moments. This intrachain antiferromagnetic arrangement is thus closer to the $S = 1/2$ antiferromagnetic intrachain coupling encountered in $CsCoCl_3$ rather than to the ferromagnetic coupling between $S = 3/2$ and $S = 1/2$ alternated moments in the chains of Ca_3CoRhO_6.

PDA-like characteristic

Despite the different high-temperature magnetic properties of Sr_3NiIrO_6, the latter exhibits several properties at low temperature reminiscent of that encountered in Ca_3CoRhO_6, Ca_3CoIrO_6 and $Ca_3Co_2O_6$. This can be seen on the $\chi(T)$ curves collected for different magnetic field values ($\mu_0 H \leq 5$ T) and by field-cooling (fc) or zero-field-cooling (zfc) (Fig. 2). Starting from the high temperature part, χ remains field independent down to 70 K. This temperature is defined as T_1 and corresponds to the setting of the antiferromagnetic interchain coupling [2]. As the temperature is further decreased, below about $T_2 = 21$ K, the $\chi_{\rm zfc}$ starts to drop, independently of the applied magnetic field value, to reach the same small magnetic susceptibility value ($\chi_{5\rm K} = 6.5 \times 10^{-3}$ emu mol^{-1}). This shape of curve with two characteristic temperatures, T_1 and T_2, has also been reported for Ca_3CoRhO_6 which is the first $A_3BB'O_6$ compound claimed to adopt a PDA state [7]. By considering this PDA state, the field independent $\chi_{5\rm K}$ value was explained as the setting of a frozen PDA-state (*f*-PDA) below T_2. In the 1/3 magnetically incoherent chain of the PDA state, the magnetic moments are believed to freeze as temperature decreases below T_2. Similarly to the *f*-PDA of Ca_3CoRhO_6 characterized with pulsed magnetic field [14], for $T \ll T_2$, the *f*-PDA state is also very stable in the case of Sr_3NiIrO_6.More than 22 T are required, at 15 K *i.e.* only 6 K below T_2, to induce a magnetic transition (Fig. 3a), indicating that at least a part of the moments have been unfrozen in an irreversible manner. It should be mentioned that the magnetization value in 35 T reaches a maximum of only 0.5 μ_B/f.u. of Sr_3NiIrO_6. The critical field of this transition decreases as the temperature approaches T_2 as shown for $T = 17.5$ K and then the transition becomes smoother as the temperature becomes closer to T_2. The alignment of the frozen moments along the field direction is thus thermally assisted. The $M(H)$ curves, obtained by an extraction method within a static field reaching up to 9 T, recorded at 25 K and 12 K for Ca_3CoRhO_6 and Sr_3NiIrO_6 exhibit very similar shapes (Fig. 3b) suggesting that these compounds are in the same background magnetic state referred as *f*-PDA in Ca_3CoRhO_6. It should be emphasized that there exists a large difference between pulsed and static magnetic fields on the $M(H)$ curves (see for instance the enlargement of Fig. 3c). This demonstrates that the dynamic of the spins is in the same range of magnitude as the time scale of our measurements.

Spin dynamics in the 'f-PDA state' ($T < T_2$)

In order to reveal the slow dynamics of the spins in the frozen state, ac-χ magnetic susceptibility measurements have been performed by using several frequencies in the range 10 to 10^3 Hz (Fig. 4). From those curves, it is found that, as the frequency (f) increases, the temperature T_f of the magnetic susceptibility peak shifts up and that the χ maximum value, at T_f, decreases. A similar temperature shift with the frequency is also found on the $\chi''(T)$ curves. Despite this behavior mimics that of a spin glass (SG), the shift of T_f with f, qualified by $K = \frac{\Delta T_f}{T_f \times \Delta \log f}$ [15], is very large with $K \sim 0.12$ for Sr_3NiIrO_6, in comparison to $K \sim 10^{-2}$ in typical SG. Such a high value is encountered in superparamagnets ($K \sim 0.3$ [15]) and is very similar to those reported in $Ca_3Co_2O_6$, $K = 0.17$ [5], and in Ca_3CoRhO_6, $K = 0.10$ [16]. The spins dynamics

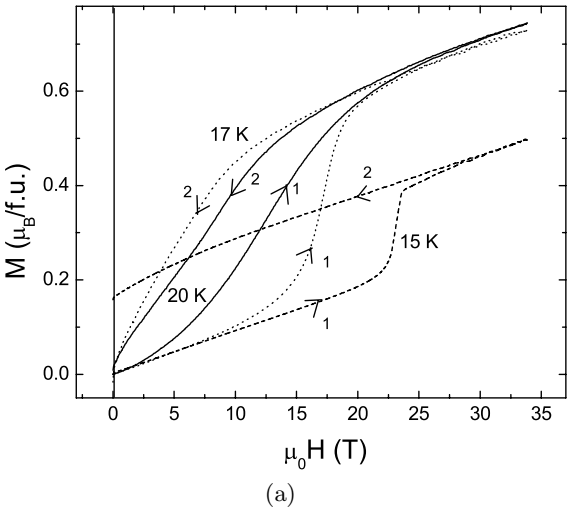

(a)

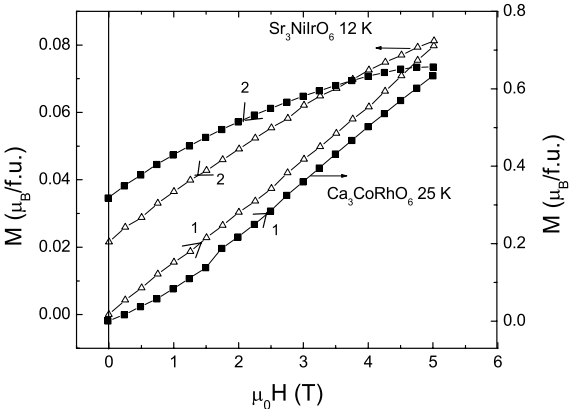

(b)

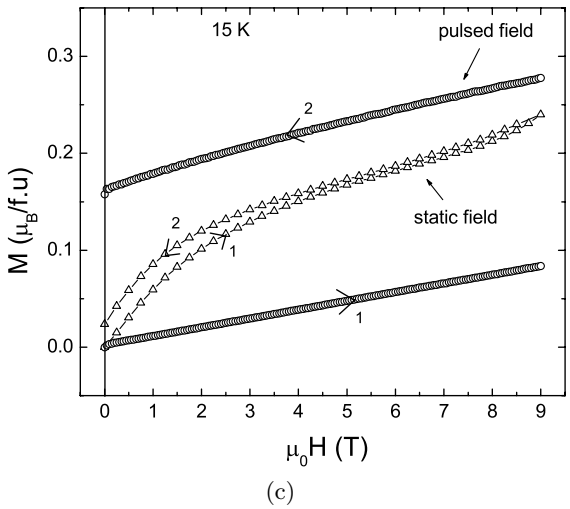

(c)

Fig. 3. Isothermal ($T < T_2$) magnetization curves for Sr_3NiIrO_6 in pulsed magnetic field (a) '1' and '2' are for the increasing and decreasing field branches, respectively. (b) The $M(H)$ (static field) collected at 25 K for Ca_3CoRhO_6 is shown with to the $M(H)_{12\ K}$ curve for Sr_3NiIrO_6. (c) Comparison between pulsed and static fields (c).

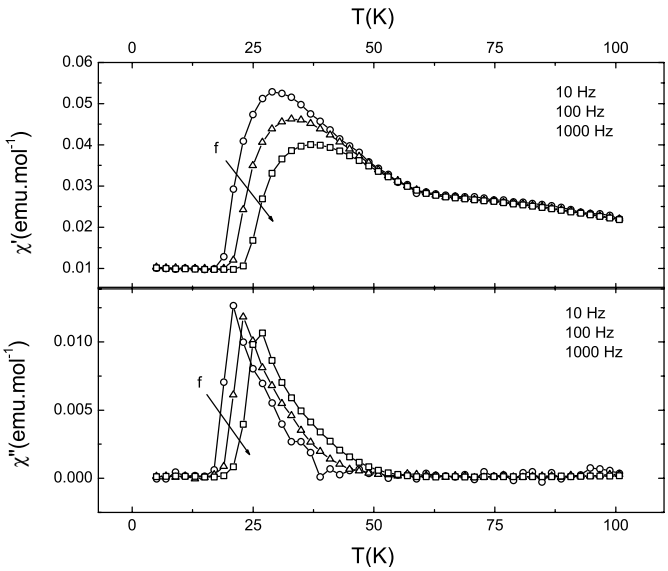

Fig. 4. Ac magnetic susceptibility (χ', χ'') as a function of T for Sr_3NiIrO_6. The frequency values are indicated.

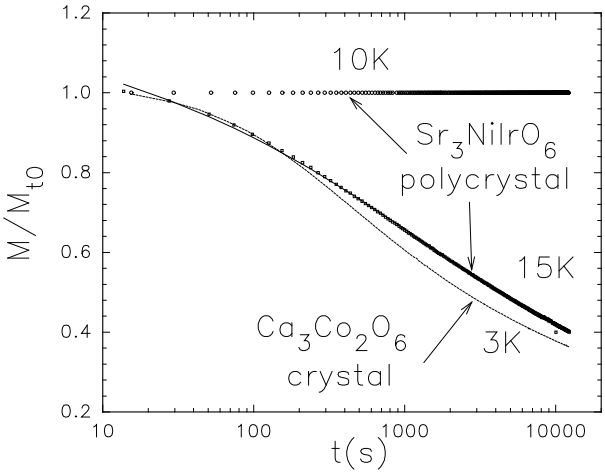

Fig. 5. Time (t) dependence of M. The sample was first field cooled in 10^{-3} T down to 15 K (or 10 K), and the $M(t)$ curve is registered after the field is returned to 0. Note that the relaxation is quasi independent on the waiting time in the field at 15 K showing an absence of aging effect. The solid line for the 15 K curve corresponds to the fitting curve (see text). A similar curve obtained at 3 K for a $Ca_3Co_2O_6$ crystal (dashed line) is also given for of comparison.

has been tested further by magnetic relaxation study. As for the K values, the magnetic relaxation is very similar in Sr_3NiIrO_6 ($T = 15$ K) and $Ca_3Co_2O_6$ ($T = 4$ K), as shown in Figure 5. The data for $Ca_3Co_2O_6$ were collected by using a single crystal with the magnetic field applied along the chain direction. The similarity of these curves shows that the polycrystalline nature of the Sr_3NiIrO_6 sample is not responsible for this feature. For Sr_3NiIrO_6, at 15 K (Fig. 5), the experimental $M(t)$ curve can be fitted by a stretched exponential, $M/M_{fc} = a + b\exp\left[-\left(\frac{t}{\tau}\right)^n\right]$, generally used for spin glasses [11,15]. From the fitting curve

with $n = 0.5$, a relaxation time τ such as $\tau = 1350$ s. is extracted, demonstrating the very slow dynamic of the spins in the frozen state. This is consistent with the *f*-PDA state proposed in reference [7]: the movement of the domain walls in the ferromagnetic chain is thermally activated and becomes extremely slow at low temperature. Accordingly, the $M(t)$ curve collected at 10 K, shows quasi no relaxation (Fig. 5) for times greater than several hours confirming that a completely frozen state is set. Now, it should be added that several different PDA phases have been predicted [17], called PDA(n) phases, where n stands for the number of different magnetic sites per magnetic unit cell. The present dynamic may also reflect the freezing of a PDA(n) phase. Furthermore, as the temperature decreases below T_2, since the interchain coupling dominates, the triangular frustration is increased. As a consequence, one could also expect that the background state is made of different ferrimagnetic domains which size decreases as T decreases. Thus, the PDA phase for $T > T_2$ would be transformed in multi-ferrimagnetic domains below T_2. Accordingly, the slow dynamic could be the result of the fluctuations of those domains characterized by a freezing temperature.

Magnetization plateau ($T_2 \leq T \leq T_1$) and nature of the intrachain coupling

In Ca_3CoRhO_6, in the temperature range where the PDA state is set ($T_2 \leq T \leq T_1$), the isothermal field dependent magnetization [$M(H)$] curves are characterized by a first magnetization plateau, as the magnetic field increases from zero, corresponding to the PDA to 'ferrimagnetic' transition. In the ferrimagnetic state, on each triangle made of three ferromagnetic chains, two chains are antiferromagnetic so that the net magnetization is only 1/3 of the values reached when the all three chains are ferromagnetic. Although the PDA state in Sr_3NiIrO_6 was not revealed by the neutron powder study performed for $T = 30$ K [10], *i.e.* in between T_2 and T_1, a clear magnetization plateau is revealed from the $M(H)$ curves (Fig. 6a). Furthermore, for the field values beyond ~7 T, the magnetization starts to increase rapidly so that the magnetization departs from the plateau. These measurements made in static magnetic fields have been completed by those made within pulsed magnetic fields (Fig. 6b). In the common range of magnetic field values, the two curves are superimposed showing that the spins dynamics has changed compared to $T \ll T_2$ and thus that the spins are able to follow the field sweep of the pulsed fields. However, these $M(H)$ curves differ strongly from those reported for $Ca_3Co_2O_6$ and Ca_3CoRhO_6. First, the magnetization values on the plateau, are close to only ~0.16 μ_B per formula unit of Sr_3NiIrO_6. If one considers the spin states, H.S. Ni^{2+} ($S = 1$) and L.S. Ir^{4+} ($S = 1/2$), one obtains $M = 3$ μ_B/f.u. for the magnetization of the three ferromagnetic chains, from which it derives $M = 1$ μ_B/f.u. for the ferrimagnetic state, *i.e.* a value six times larger than the experimental value observed on the magnetization plateau for Sr_3NiIrO_6. The second important point deals

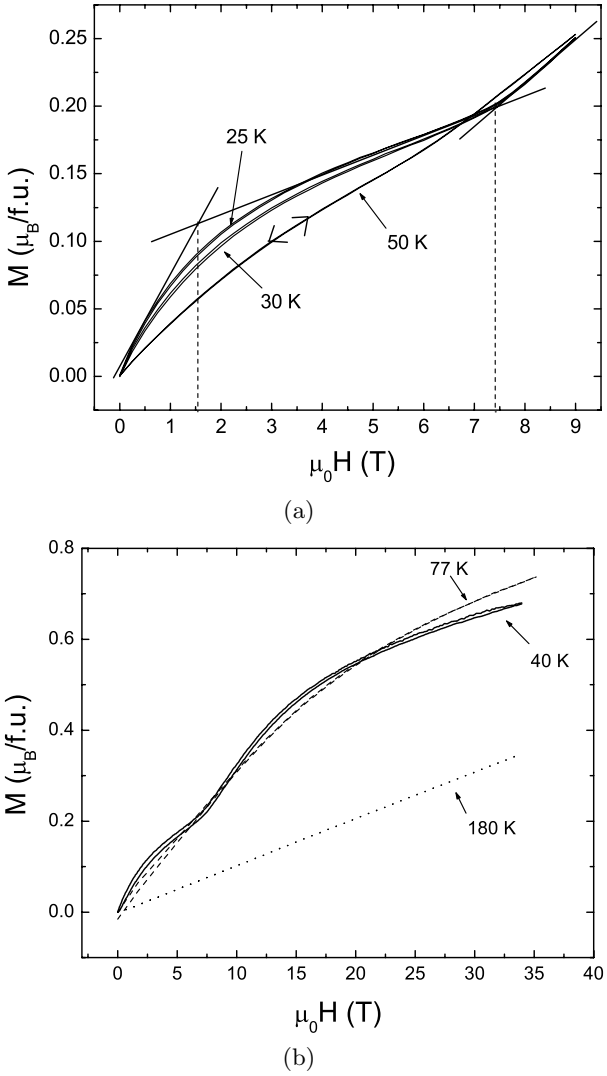

Fig. 6. Isothermal $M(H)$ curve of Sr_3NiIrO_6 for $T > T_2$. T values are labelled on the graph. (a) static fields; (b) pulsed magnetic fields. In Figure 6a, the intersections of the two sets of lines show how the characteristic magnetic fields are taken to build the diagram of Figure 7.

with the lack of saturation for the magnetization even in 35 T. In the other compounds, such as Ca_3CoRhO_6, the magnetization ratio between ferri- and ferromagnetic configurations verifies the 1/3 expected value. In contrast, for Sr_3NiIrO_6, the magnetization value at 35 T is larger than the product $3 \times M_{\text{ferri}} \approx 0.5$ μ_B/f.u. This outlines the different behavior of Sr_3NiIrO_6.

In order to try to interpret this difference, one must consider the isotropic magnetic nature of this polycrystalline Sr_3NiIrO_6 sample which forbids a complete alignment of the chain magnetization upon the magnetic field direction. To try to overcome this difficulty, a mixture of Sr_3NiIrO_6 powder and grease has been submitted to a 9 T field at 320 K and then cooled down to 80 K. At this stage, the field was finally removed. However, no change was obtained on the subsequent $M(H)$ curves, for

$T_1 < T < T_2$, whereas, for the same process, a clear grain alignment, with the magnetization of the chains parallel to the field direction, is achieved in the case of a powder of a polycrystalline $Ca_3Co_2O_6$ sample [4]. This lack of alignment under magnetic field is consistent with the low magnetic susceptibility of Sr_3NiIrO_6 which, at 300 K, is three times smaller than that of $Ca_3Co_2O_6$. This also strongly supports that the intrachain magnetic coupling in Sr_3NiIrO_6 is antiferromagnetic contrasting with the ferromagnetic one in the case of $Ca_3Co_2O_6$. Furthermore, the different high-temperature behavior of the inverse magnetic susceptibility, with $\theta_p = -61$ K and a different curvature of the $\chi^{-1}(T)$ curve at high temperature, compared for instance to Ca_3CoRhO_6, indicates that the intrachain magnetic coupling is antiferromagnetic with opposite directions for the Ni^{2+} and Ir^{4+} magnetic moments. Then, one would expect 0.33 μ_B/f.u. for the ferrimagnetic configuration on the triangle, *i.e.* two chains over three are antiferromagnetically coupled. In reference [4], the alignment of the $Ca_3Co_2O_6$ crystallites under magnetic field, makes the magnetization increasing by a factor 1.6 compared to that of a randomly dispersed powder. If the Ni^{2+} and Ir^{4+} magnetic moments were ferromagnetically coupled, such a factor would not be sufficient to reach the expected value of $3\mu_B$/f.u. for the ferromagnetic configuration on the triangle. These results are thus in agreement with the intrachain antiferromagnetic coupling for Sr_3NiIrO_6 which contrasts with the intrachain ferromagnetic coupling reported for $Ca_3Co_2O_6$, Ca_3CoRhO_6 and Ca_3CoIrO_6. As a consequence, when the field increases beyond the critical field of the transition from the ferrimagnetic to ferromagnetic state for the chains on the triangular lattice, not only the magnetization of the 1/3 antiparallel chain will reverse, but also the opposite moments to the field in the chains will also tend to flip. Two ferri- to ferromagnetic transitions occur in Sr_3NiIrO_6, the interchain and intrachain ones.

Discussion and concluding remarks

The present magnetic study of the Sr_3NiIrO_6 compound confirms the existence of features basically similar to those of a partially disordered antiferromagnetic (PDA) state. Furthermore, there exists also for this compound, as for Ca_3CoIrO_6, Ca_3CoRhO_6 and $Ca_3Co_2O_6$, a frozen disordered state (*f*-PDA), below $T_2 = 21$ K. For $T \ll T_2$, the magnetic moments are totally blocked or respond very slowly to the excitation magnetic field as T approaches T_2. This spins dynamic could be associated to a loss of magnetic coherence along the "Ni-O-Ir" chains as the temperature decreases from T_2. This suggests that short magnetic links in the chain are formed at low temperature which are responsible for the peculiar dynamic of this spins system. In this respect, the triangular geometrical frustration plays most probably a crucial role, as discussed in the theoretical paper on the PDA state [6]. Alternatively, the transition from a PDA(n) state ($T > T_2$) to multiferrimagnetic domains below T_2 could also provide similar features from the dynamical point of view, with fluctuations and freezing of these magnetic domains responsible for a slow dynamic and a T_g, respectively. Nevertheless, the PDA-like features of Sr_3NiIrO_6 are thus in apparent contradiction with the lack of antiferromagnetic peaks on the neutron diffraction patterns reported for Sr_3NiIrO_6 at 30 K [10].

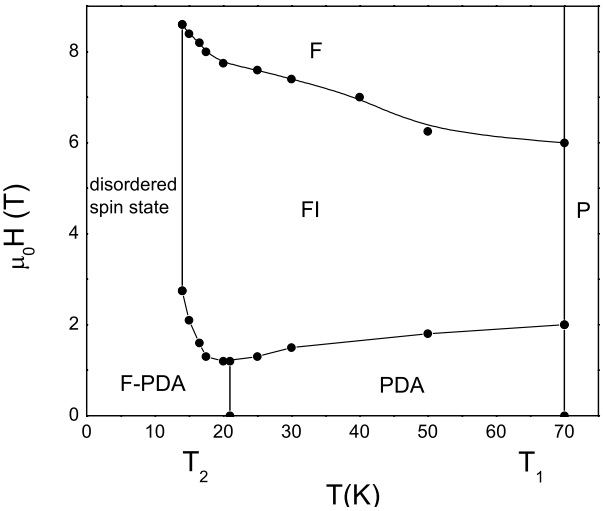

Fig. 7. Schematic (T, H) phase diagram of Sr_3NiIrO_6. F = ferromagnetic; FI: ferrimagnetic; PDA and f-PDA are for the partially disordered antiferromagnetic state and the frozen-PDA; P: Paramagnetic.

Finally, a phase diagram can be proposed for Sr_3NiIrO_6 (Fig. 7). According to the very slow spin dynamic below T_2, this diagram is built only on the basis of the static field magnetization measurements (9 T maximum field). At low temperature ($T < T_2$) and small enough magnetic field values, the sample is in a frozen disordered magnetic state whereas, for $T_1 < T < T_2$, it is in a PDA-like state. By increasing the magnetic field, the magnetic state evolves towards the ferrimagnetic state on the triangle characterized by a magnetization plateau for $T_1 < T < T_2$. The characteristic magnetic field of this transition towards a ferrimagnetic (FI) state is taken by intersecting two straight lines as shown in Figure 6a. But, below T_2, the transition from disordered to FI is not as clear, and a line between these two states can be hardly drawn. Then for fields larger than about 7 T, the magnetization increases again more rapidly as to reach the ferromagnetic (F) state. Again from the crossing point of two lines, a magnetic field for the FI to F transition is obtained (Fig. 6a). But in contrast to Ca_3CoRhO_6 and $Ca_3Co_2O_6$, the magnetization in large fields (up to 35 T) does not saturate to a magnetization that would correspond to three times the M value on the FI plateau. This is consistent with the fact that these large field values tend also to make flipping the spins in the chains (intrachain ferrimagnetic to ferromagnetic transition). Sr_3NiIrO_6 is thus a unique $A_3BB'O_6$ compound exhibiting two ferri- to ferromagnetic transitions, interchain and intrachain.

References

1. H. Fjellvag, E. Gulbrandsen, S. Aasland, A. Olsen, B. Hauback, J. Solid State Chem. **124**, 190 (1996)
2. S. Aasland, H. Fjellvag, B. Hauback, Solid State Commun. **101**, 187 (1997)
3. K.E. Stitzer, J. Darriet, H-C. zur Loye, Current Opinion Solid State Mater. Sci. **5**, 535 (2001)
4. H. Kageyama, K. Yoshimura, K. Kosuge, M. Azuma, M. Takano, M. Mitamura, T. Goto, J. Phys. Soc. Jpn **66**, 3996 (1997)
5. A. Maignan, C. Michel, A.C. Masset, C. Martin, B. Raveau, Eur. Phys. J. B **15**, 657 (2000)
6. M. Mekata, J. Phys. Soc. Jpn **42**, 76 (1977); M. Mekata, K. Adachi, J. Phys. Soc. Jpn **44**, 806 (1978)
7. S. Niitaka, K. Yoshimura, H. Kageyama, K. Kosuge, M. Nishi, K. Katurai, Phys. Rev. Lett. **87**, 177202 (2001)
8. S. Niitaka, H. Kageyama, M. Kato, K. Yoshimura, K. Kosuge, J. Solid State Chem. **146**, 137 (1999)
9. H. Kageyama, K. Yoshimura, K. Kosuge, J. Solid State Chem. **140**, 14 (1998)
10. T.N. Nguyen, H.C. zur Loye, J. Solid State Chem. **117**, 300 (1995); G.V. Vajenine, R. Hoffmann, H.C. zur Loye, Chem. Phys. **204** 469 (1996)
11. E. Vincent, in: *Recent Process in Random magnets*, edited by D.H. Ryan (World Scientific, Singapore,1992)
12. J. Rodriguez-Carvajal, Physica B **192**, 55 (1993)
13. D. Jung, Ph.D. Thesis, Bordeaux I University, France (1995)
14. S. Niitaka, H. Kageyama, K. Yoshimura, K. Kosuge, S. Kawano, N. Aso, A. Mitsuda, H. Mitamura, T. Goto, J. Phys. Soc. Jpn **70**, 1222 (2001)
15. J.A. Mydosh, *Spin Glasses* (Taylor and Francis, London 1993)
16. E.V. Sampathkumaran, A. Niazi, Phys. Rev. B. **65**, 180401 (2002)
17. T. Takagi, M. Mekata, J. Phys. Soc. Jpn **64**, 4609 (1995)